Appl. Phys. B 87, 547–552 (2007)
DOI: 10.1007/s00340-007-2615-9

Applied Physics B
Lasers and Optics

X. CHU✉
Y. NI
G. ZHOU

Propagation of cosh-Gaussian beams diffracted by a circular aperture in turbulent atmosphere

School of Science, Zhejiang Forestry University, Lin'an 311300, P.R. China

Received: 26 October 2006/Revised version: 29 January 2007
Published online: 5 April 2007 •

ABSTRACT An analytical formula for the average intensity of cosh-Gaussian (ChG) beams diffracted by an aperture in turbulent atmosphere is derived and some limiting cases are discussed. By using the average intensity formula, some numerical simulation comparisons are made and some special cases are studied, especially the influences of the ChG beam parameter (Ω_0), the propagation distance, the aperture and its size on the average normalized intensity distribution. It is determined that the evolution properties of the average normalized intensity profile in turbulent atmosphere with aperture are different not only from those of free space with aperture but also from those in turbulent atmosphere without aperture.

PACS 42.68.Bz; 42.79.Ag; 42.25.Fx

1 Introduction

Hermite-sinusoidal-Gaussian (HSG) beams were introduced by Casperson et al. and a comprehensive study of HSG beam theory has been given [1–3]. Since then the properties of HSG beams have attracted much attention and several related studies have appeared in the literature [4–8]. In fact, the HSG beams represent the more general beams. A Gaussian beam, a Hermite–Gaussian beam, a cosh-Gaussian (ChG) beam and a sinh-Gaussian beam can be regarded as special cases of them. Among the sets of HSG beams, the ChG beams have some important applications; for example, ChG dependence exhibits a concentration of energy in the outer lobes of a beam that can be used in the space diversity applications in free-space optics (FSO) systems. In addition, their profiles can also resemble closely the flat-topped field distributions by a suitable choice of beam parameters. Their production and propagation in free space with or without a hard-edge aperture have been studied [9–11].

A laser beam propagating in the atmosphere will be affected by turbulence. It will cause distortions in the intensity, phase, angle of arrival and displacement of the laser beam at the observation plane. With the wide applications of laser beams in the atmosphere, various theoretical models have been proposed to describe the effects of turbulence on the induced image degradation and intensity fluctuations [12–16]. Much work has been carried out concerning the propagation of a laser beam in turbulent atmosphere. In particular, Eyyuboğlu and Baykal presented the reciprocity of cos-Gaussian and cosh-Gaussian beams [17] and the average intensity of cosh-Gaussian beams in turbulent atmosphere [18]. Eyyuboğlu investigated the propagation of Hermite-cos-Gaussian [19] and Hermite-cosh-Gaussian [20] laser beams in turbulent atmosphere. Cai and He studied the propagation of various dark hollow beams in turbulent atmosphere [21]. However, these studies have been restricted to the unapertured cases.

In practice, the aperture effect exists more or less. On the one hand, the diffraction by an aperture ultimately determines the limiting resolution in an optical system. But, on the other hand, diffraction by an aperture could control the propagation of laser beams. It is hoped that the propagation rules of laser beams limited by an aperture could promote the application of laser beams in turbulent atmosphere, such as optical communication, phased arrays and optical super-resolution. In this paper, our center of interest is on ChG beam propagation in turbulent atmosphere limited by an aperture. The relations between the average intensity and the propagation distance, the size of the aperture and the parameters of the ChG beam will redound to the applications of a ChG beam propagating in turbulent atmosphere.

2 The average intensity of ChG beam diffracted by an aperture in turbulent atmosphere

In the Cartesian coordinate system, the field of ChG beams propagating in free space along the z-axis is given by [1]

$$E_0(x, y, 0) = \exp\left(-\frac{x^2+y^2}{w_0^2}\right)\cosh(\Omega_0 x)\cosh(\Omega_0 y)\,, \quad (1)$$

where w_0 is the waist width of the Gaussian amplitude distribution and Ω_0 is the parameter associated with the cosh part. Assume that, as shown in Fig. 1, an aperture with radius a is located at the source plane ($z = 0$), and the receiver plane is located at the z-plane. Here, (x, y) and (p, q) denote the transverse coordinates of the source and the receiver, respectively.

✉ Fax: +86 551 2199050, E-mail: chuxiuxiang@yahoo.com.cn

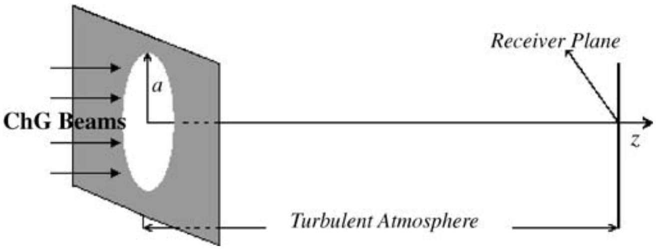

FIGURE 1 Propagation geometry

The field just behind the aperture reads

$$E(x,y,0)=t(x,y)\exp\left(-\frac{x^2+y^2}{w_0^2}\right)\cosh(\Omega_0 x)\cosh(\Omega_0 y)\,, \tag{2}$$

where the window function $t(x, y)$ of the hard-edge aperture is written as

$$t(x,y)=\begin{cases}1\,, & x^2+y^2\le a^2\,,\\ 0\,, & \text{otherwise.}\end{cases} \tag{3}$$

According to the extended Huygens–Fresnel principle, the average intensity at the z-plane can be expressed as [17]

$$\begin{aligned}&\langle I(p,q,z)\rangle\\ &=\frac{k^2}{(2\pi z)^2}\int\limits_{-\infty}^{\infty}\int\limits_{-\infty}^{\infty}\int\limits_{-\infty}^{\infty}\int\limits_{-\infty}^{\infty} E(x,y,0)E^*(\xi,\eta,0)\\ &\quad\times\exp\left\{\frac{\mathrm{i}k}{2z}\left[(p-x)^2+(q-y)^2-(p-\xi)^2-(q-\eta)^2\right]\right\}\\ &\quad\times\langle\exp[\psi(x,y,p,q)+\psi^*(\xi,\eta,p,q)]\rangle\,\mathrm{d}x\,\mathrm{d}y\,\mathrm{d}\xi\,\mathrm{d}\eta\,,\end{aligned} \tag{4}$$

where k is the wave number, the asterisk $(*)$ denotes complex conjugation and $\langle\ \rangle$ indicates the ensemble average over the medium's statistics covering the log-amplitude and phase fluctuations due to the turbulent atmosphere. $\psi(x, y, p, q)$, the solution to the Rytov method, represents the random part of the complex phase of a spherical wave that propagates from the source point $(x, y, 0)$ to the receiver point (p, q, z). The ensemble average term within the integrand of (4) is [22]

$$\begin{aligned}&\langle\exp[\psi(x,y,p,q)+\psi^*(\xi,\eta,p,q)]\rangle\\ &=\exp[-0.5D_\psi(x-\xi,y-\eta)]\\ &=\exp\left\{-\frac{1}{\varrho_0^2}\left[(x-\xi)^2+(y-\eta)^2\right]\right\}\,,\end{aligned} \tag{5}$$

where $D_\psi(x-\xi, y-\eta)$ is the wave structure function, $\varrho_0 = (0.545C_n^2k^2z)^{-3/5}$ is the coherence length of a spherical wave that propagates in the turbulent medium and C_n^2 is the structure constant. As the wave structure function is approximated by the phase structure function, Rytov's phase structure function is used here. It is valid not only in the case of weak turbulence, but also in the case of strong turbulence [23]. In order to obtain a simple and analytical formula, a Kolmogorov spectrum and a quadratic approximation of the 5/3 power law for Rytov's phase structure function are also employed. By substituting (2) and (5) into (4), the average intensity at the receiver plane becomes

$$\begin{aligned}&\langle I(p,q,z)\rangle\\ &=\frac{k^2}{(2\pi z)^2}\int\limits_{-\infty}^{\infty}\int\limits_{-\infty}^{\infty}\int\limits_{-\infty}^{\infty}\int\limits_{-\infty}^{\infty} t(x,y)E_0(x,y,0)t^*(\xi,\eta)E_0(\xi,\eta,0)\\ &\quad\times\exp\left(\frac{\mathrm{i}k}{2z}\left[(p-x)^2+(q-y)^2-(p-\xi)^2-(q-\eta)^2\right]\right)\\ &\quad\times\exp\left(-\frac{1}{\varrho_0^2}\left[(x-\xi)^2+(y-\eta)^2\right]\right)\mathrm{d}x\,\mathrm{d}y\,\mathrm{d}\xi\,\mathrm{d}\eta\,.\end{aligned} \tag{6}$$

In order to obtain the analytical expression of the average intensity, we first expand the hard-edge aperture function as the sum of complex Gaussian functions with finite terms [24]:

$$t(x,y)=\sum_{j=1}^{m}B_j\exp\left[-\frac{C_j}{a^2}(x^2+y^2)\right]\,, \tag{7}$$

where the complex constants B_j and C_j are the expansion coefficients that can be obtained by optimization computation directly [25]. If we insert (7) into (6) and assume that

$$\begin{aligned}f(p,z)=&\int\limits_{-\infty}^{\infty}\int\limits_{-\infty}^{\infty}\exp\left[-\left(\frac{1}{w_0^2}+\frac{C_j}{a^2}\right)x^2\right]\cosh(x)\\ &\times\exp\left[-\left(\frac{1}{w_0^2}+\frac{C_s^*}{a^2}\right)\xi^2\right]\cosh(\xi)\\ &\times\exp\left(\frac{\mathrm{i}k}{2z}\left[(p-x)^2-(p-\xi)^2\right]\right)\\ &\times\exp\left[-\frac{1}{\varrho_0^2}(x-\xi)^2\right]\mathrm{d}x\,\mathrm{d}\xi\,,\end{aligned} \tag{8}$$

(6) can be expressed as

$$\langle I(p,q,z)\rangle=\frac{k^2}{(2\pi z)^2}\sum_{j=1}^{m}\sum_{s=1}^{m}B_jB_s^*f(p,z)f(q,z)\,. \tag{9}$$

By using the integral formula [26]

$$\int\limits_{-\infty}^{\infty}\exp(-p^2x^2\mp qx)\,\mathrm{d}x=\frac{\sqrt{\pi}}{p}\exp\left(\frac{q^2}{4p^2}\right)\,, \tag{10}$$

(8) can be expressed as

$$\begin{aligned}f(p,z)=&\frac{\pi\varrho_0^2}{4\sqrt{\beta_1\beta_2\varrho_0^4-1}}\\ &\times\left\{\left[\exp\left(\frac{\beta_1\varrho_0^4\alpha_1^2}{4\beta_1\beta_2\varrho_0^4-4}\right)+\exp\left(\frac{\beta_1\varrho_0^4\alpha_2^2}{4\beta_1\beta_2\varrho_0^4-4}\right)\right]\right.\\ &\times\exp\left[\frac{1}{4\beta_1}\left(\Omega_0-\frac{\mathrm{i}k}{z}t\right)^2\right]\\ &+\left[\exp\left(\frac{\beta_1\varrho_0^4\alpha_3^2}{4\beta_1\beta_2\varrho_0^4-4}\right)+\exp\left(\frac{\beta_1\varrho_0^4\alpha_4^2}{4\beta_1\beta_2\varrho_0^4-4}\right)\right]\\ &\left.\times\exp\left[\frac{1}{4\beta_1}\left(\Omega_0+\frac{\mathrm{i}k}{z}t\right)^2\right]\right\}\,,\end{aligned} \tag{11}$$

where

$$\beta_1=\frac{1}{w_0^2}+\frac{1}{\varrho^2}+\frac{C_g^*}{a^2}-\frac{\mathrm{i}k}{2z}\,, \tag{12}$$

$$\beta_2=\frac{1}{w_0^2}+\frac{1}{\varrho^2}+\frac{C_j}{a^2}-\frac{\mathrm{i}k}{2z}\,, \tag{13}$$

$$\alpha_1=\frac{\mathrm{i}kp}{z}\left(1-\frac{1}{\beta_1\varrho^2}\right)-\left(1-\frac{1}{\beta_1\varrho^2}\right)\Omega_0\,, \tag{14}$$

$$\alpha_2=\frac{\mathrm{i}kp}{z}\left(1-\frac{1}{\beta_1\varrho^2}\right)+\left(1+\frac{1}{\beta_1\varrho^2}\right)\Omega_0\,, \tag{15}$$

$$\alpha_3=\frac{\mathrm{i}kp}{z}\left(1-\frac{1}{\beta_1\varrho^2}\right)-\left(1+\frac{1}{\beta_1\varrho^2}\right)\Omega_0\,, \tag{16}$$

$$\alpha_4=\frac{\mathrm{i}kp}{z}\left(1-\frac{1}{\beta_1\varrho^2}\right)+\left(1-\frac{1}{\beta_1\varrho^2}\right)\Omega_0\,. \tag{17}$$

From (9) and (11)–(17), the average intensity at an arbitrary position for a ChG beam diffracted by an aperture in turbulent atmosphere can be obtained. As the series is finite, a more convenient method is provided to investigate the average intensity of ChG beams with aperture in turbulent atmosphere. If we set $a\to\infty$, from (9) the average intensity of ChG beams without aperture in turbulent atmosphere can be obtained:

$$\langle I(p,q,z)\rangle=\frac{k^2}{(2\pi z)^2}f(p,z)f(q,z)\,. \tag{18}$$

From (11)–(17), $f(p,z)$ within (18) can be simplified to

$$\begin{aligned}f(p,z)=&\frac{\pi\varrho_0 z w_0^2}{2\sqrt{8z^2w_0^2+k^2w_0^4\varrho_0^2+4z^2\varrho_0^2}}\\&\times\left\{2\exp\left[\frac{2\varrho_0^2w_0^2\left(\Omega_0^2z^2-k^2p^2\right)}{8z^2w_0^2+k^2w_0^4\varrho_0^2+4z^2\varrho_0^2}\right]\right.\\&\times\cos\left(\frac{4kz\Omega_0\varrho_0^2w_2^2p}{8z^2w_0^2+k^2w_0^4\varrho_0^2+4z^2\varrho_0^2}\right)\\&+\exp\left[\frac{2w_0^2\left(2\Omega_0^2w_0^2z^2+\Omega_0^2z^2\varrho_0^2-k^2\varrho_0^2p^2\right)}{8z^2w_0^2+k^2w_0^4\varrho_0^2+4z^2\varrho_0^2}\right]\\&\times\left[\exp\left(\frac{2k^2\Omega_0\varrho_0^2w_2^4p}{8z^2w_0^2+k^2w_0^4\varrho_0^2+4z^2\varrho_0^2}\right)\right.\\&\left.\left.+\exp\left(\frac{-2k^2\Omega_0\varrho_0^2w_2^4p}{8z^2w_0^2+k^2w_0^4\varrho_0^2+4z^2\varrho_0^2}\right)\right]\right\}.\end{aligned} \tag{19}$$

Here, we point out that in our paper the cosh part ($\cosh(ax)\times\cosh(ay)$) is in disagreement with the cosh part ($\cosh(ax+by)$) in [18]. Since $\cosh(ax)\cosh(ay)=0.5[\cosh(ax-ay)+\cosh(ax+ay)]$, we can obtain (18) and (19) of our paper from (17) of [18]. Study shows that (18) and (19) agree with (17) of [18]. From (18) and (19) and setting $\Omega_0=0$, the average intensity of Gaussian beams without aperture in turbulent atmosphere can be expressed as

$$\begin{aligned}\langle I(p,q,z)\rangle=&\frac{k^2w_0^4\varrho^2}{k^2w_0^4\varrho^2+4z^2\left(2w_0^2+\varrho^2\right)}\\&\times\exp\left[-\frac{2k^2w_0^2\varrho^2(p^2+q^2)}{k^2w_0^4\varrho^2+4z^2\left(2w_0^2+\varrho^2\right)}\right].\end{aligned} \tag{20}$$

Equation (20) is in accordance with the existing results of Gaussian beams without aperture in turbulent atmosphere [17, 18].

If we set $\varrho_0\to\infty$, (19) can be simplified to

$$\begin{aligned}f(p,z)=&\frac{\pi z w_0^2}{2\sqrt{k^2w_0^4+4z^2}}\\&\times\exp\left[\frac{2w_0^2\left(k^2p^2+k^2\Omega_0w_0^2p-\Omega_0^2z^2\right)}{k^2w_0^4+4z^2}\right]\\&\times\left\{1+\exp\left[\frac{4k^2\Omega_0w_0^4p}{k^2w_0^4+4z^2}\right]\right.\\&\left.+2\exp\left[\frac{2k^2\Omega_0w_0^4p}{k^2w_0^4+4z^2}\right]\cos\left(\frac{4kz\Omega_0w_2^2p}{k^2w_0^4+4z^2}\right)\right\}.\end{aligned} \tag{21}$$

Equations (18) and (21) are the expressions of the intensity of ChG beams without aperture in free space. It should be pointed out that the analytical formula (9) is an approximate analytical expression by using a sum of finite-term complex Gaussian functions to express a hard-edge aperture. The studies [26, 27] showed that the method can provide satisfactory results in the far field. For example, the Fresnel number $F_w\le 1$ ($F_w=w_0^2/\lambda z$), the error being less than 1%. But, the error increases with increasing Fresnel number. For example, for a Fresnel number $F_w=7$, the error can reach 10%. However, for the limiting cases, (18)–(21) are precise expressions.

3 Numerical calculation results and analyses

In order to study the variation of the average intensity of ChG beams diffracted by an aperture in turbulent atmosphere with different parameters, some numerical simulations are performed. Here, we choose the deuterium fluoride (DF) chemical laser mid-infrared wavelength ($\lambda=3.8\times10^{-6}$ m). Because the circular aperture and the ChG beams at the source plane adopted in this paper are x–y symmetric, the average intensity distributions at the receiver plane are x–y symmetric. The properties of one-dimensional intensity distributions can reflect the properties of a two-dimensional intensity distribution. Therefore, we adopt one-dimensional intensity distributions in the following numerical calculation and analysis. Here, we define the one-dimensional average normalized intensity as

$$\langle J_p(p,z)\rangle=\frac{\langle I_p(p,z)\rangle}{P_0(0)}\,, \tag{22}$$

$$P_0(0)=\int_{-\infty}^{\infty}E_0^2(x,0)\,\mathrm{d}x=\frac{\sqrt{2\pi}w_0}{4}\left[\exp\left(\frac{w_0^2\Omega_0^2}{2}\right)+1\right], \tag{23}$$

where $\langle J_p(p,z)\rangle$ is the one-dimensional average normalized intensity and $P_0(0)$ is the incident power of the ChG beams. Without aperture, $\langle I_p(p,z)\rangle$ can be expressed as

$$\langle I_p(p,z)\rangle=\frac{k}{2\pi z}f(p,z) \tag{24}$$

and $\langle J_p(p,z)\rangle$ satisfies the equation

$$\int_{-\infty}^{\infty} J_p(p,z)\,\mathrm{d}p = 1\,. \tag{25}$$

Within (24), $f(p,z)$ is in the form of (19). With aperture, $\langle I_p(p,z)\rangle$ can be expressed as

$$\langle I_p(p,z)\rangle = \frac{k}{2\pi z}\sum_{j=1}^{m}\sum_{s=1}^{m} B_j B_s^* f(p,z)\,. \tag{26}$$

Within (24), $f(p,z)$ is in the form of (11)–(17). Figure 2 represents the one-dimensional average normalized intensity distribution for different Ω_0 with $w_0 = 0.1$ m at the input plane just before the aperture, where

$$J_{0x}(x,0) = \frac{E_{0x}(x,0)}{P_0(0)}\,, \tag{27}$$

$$E_{0x}(x,0) = \exp\left(-\frac{x^2}{w_0^2}\right)\cosh(\Omega_0 x)\,. \tag{28}$$

From Fig. 2 and in order to compare with Fig. 1a in [10], we can see that for a small value of Ω_0, the one-dimensional average normalized intensity profile of the ChG beam is similar to a Gaussian distribution (without a central dip) and, with Ω_0 increasing, the profile becomes flat-topped ($\Omega_0 = 14.4\,\mathrm{m}^{-1}$). Moreover, with Ω_0 further increasing, the central dip appears, and becomes larger and deeper. In order to compare with the one-dimensional average normalized intensity profiles at the z-plane of the ChG beam diffracted by an aperture in turbulent atmosphere, the one-dimensional average normalized intensity distribution $\langle J_p(p,z)\rangle$ versus different Ω_0 with $C_n^2 = 10^{-14}\,\mathrm{m}^{-2/3}$, $w_0 = 0.1$ m and $\lambda = 3.8\times10^{-6}$ m for the unapertured case are represented (calculated by (24) and (19)), as shown in Fig. 3. Meanwhile, under the same conditions of Fig. 3, the one-dimensional average normalized intensity profiles at the z-plane ($z = 8\times10^3$ m) of ChG beams diffracted by an aperture ($a = 0.1$ m) are shown in Fig. 4 (calculated by (26) and (11)–(17)).

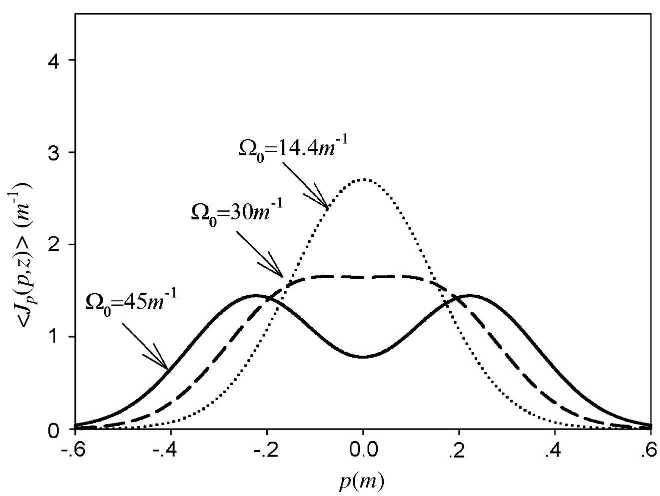

FIGURE 3 One-dimensional average normalized intensity distributions of ChG beams with different Ω_0 for unapertured case at the z-plane, where $z = 8\times10^3$ m, $\lambda = 3.8\times10^{-6}$ m and $C_n^2 = 10^{-14}\,\mathrm{m}^{-2/3}$

From Figs. 2 and 3 and on comparing with Fig. 1c in [10], we can see that the evolution properties of the one-dimensional average normalized intensity profile in turbulent atmosphere are different from those in free space. In turbulent atmosphere, the one-dimensional average normalized intensity profile of the ChG beam at the z-plane ($z = 8\times10^3$ m) has changed much compared with the profile at the input plane. Namely, for a small value of Ω_0 ($\Omega_0 = 14.4\,\mathrm{m}^{-1}$), the flat-topped profile disappears and becomes a profile that bears some resemblance to the intensity profile of a Gaussian beam (see the dotted lines in Figs. 2 and 3). For $\Omega_0 = 30\,\mathrm{m}^{-1}$, the central dip of the normalized intensity profile at the z-plane disappears and becomes flat-topped (see the dashed lines in Figs. 2 and 3). For $\Omega_0 = 45\,\mathrm{m}^{-1}$, the central dip begins to disappear (see the solid lines in Figs. 2 and 3). Meanwhile, the peak values of the one-dimensional average normalized intensity at the z-plane all decrease.

Figures 3 and 4 show that the one-dimensional normalized intensity profile is affected little by the aperture for a small

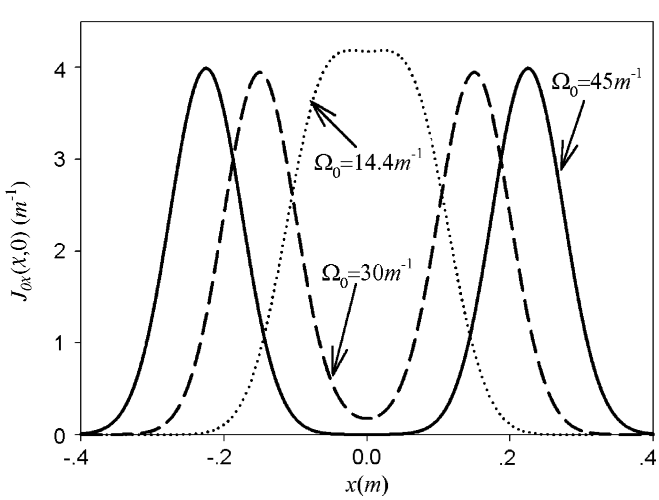

FIGURE 2 One-dimensional average normalized intensity distributions of ChG beams at the input plane just before the aperture, where $w_0 = 0.1$ m

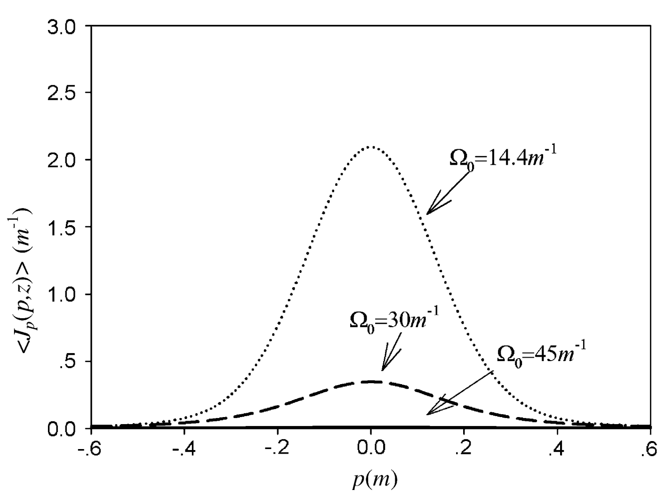

FIGURE 4 One-dimensional average normalized intensity distributions of ChG beams with an aperture with different Ω_0 at the z-plane, where $a = 0.1$ m, $z = 8\times10^3$ m, $\lambda = 3.8\times10^{-6}$ m and $C_n^2 = 10^{-14}\,\mathrm{m}^{-2/3}$

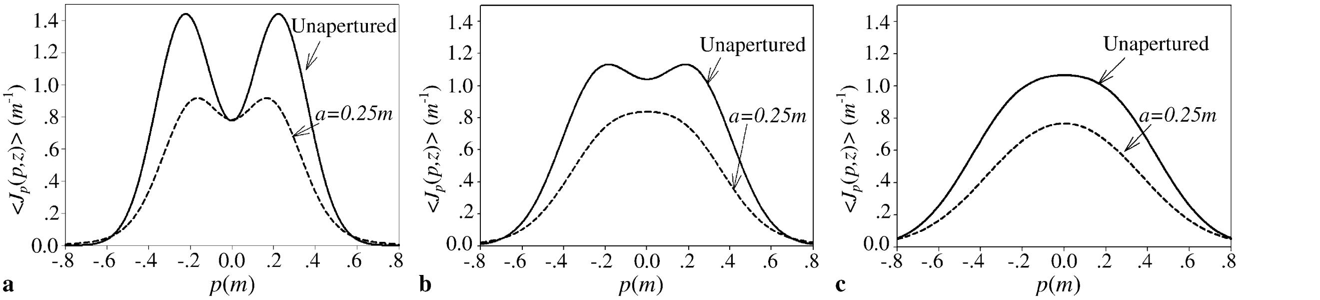

FIGURE 5 One-dimensional average normalized intensity distributions of ChG beams with different propagation distance, where $\Omega_0 = 45\ \mathrm{m}^{-1}$, $\lambda = 3.8 \times 10^{-6}$ m and $C_n^2 = 10^{-14}\ \mathrm{m}^{-2/3}$

value of Ω_0 but, with the value of Ω_0 increasing, the effect due to the aperture increases greatly. For example, the one-dimensional average normalized intensity profile for $\Omega_0 = 45\ \mathrm{m}^{-1}$ in Fig. 4 is hardly seen. This is because the peaks' span of the intensity distribution of the incident ChG beams for $\Omega_0 = 45\ \mathrm{m}^{-1}$ is so large that only little energy could pass though the aperture. Figure 5 represents the one-dimensional normalized average intensity distribution for different propagation distances with and without aperture.

From Fig. 5 we can see that the evolution properties of the one-dimensional average normalized intensity profiles with an aperture in turbulent atmosphere are similar to those for the unapertured case. Namely, the central dips disappear gradually as the propagation distance z increases. In the far field, the central dips disappear completely and the beams become Gaussian beams (without a central dip), but the conversion with an aperture is quicker than that without an aperture. However, the evolution properties of the one-dimensional average normalized intensity profiles of ChG beams propagating in turbulent atmosphere are also closely related with the radius of the aperture. Figure 6 represents the one-dimensional normalized average intensity distribution for different apertures.

Figure 6 depicts that for a small value of a, the variation of the aperture size will affect greatly the one-dimensional average normalized intensity distribution (see the dashed line in Fig. 4 and the dotted line in Fig. 6). With the value of a increasing, the one-dimensional average normalized intensity distribution is close to the unapertured case (see the dashed and solid lines in Fig. 6).

4 Conclusion

In this paper we have derived an approximate analytical formula for the average intensity of ChG beams diffracted by an aperture in turbulent atmosphere. Some limiting cases were studied. It agrees with the existing results. In order to see the properties of ChG beams with aperture in turbulent atmosphere, one-dimensional average normalized intensity profiles with different parameters have been studied and numerically calculated. It demonstrates that the propagation distance, the parameter of the ChG beams (Ω_0), the aperture and its size all affect the average intensity distributions of ChG beams propagating in turbulent atmosphere. A turbulent atmosphere could transform the intensity profiles of ChG beams to the intensity profiles of Gaussian beams (without a central dip) as the propagation distance z increases. The conversion with an aperture is quicker than that without an aperture and this process is further accelerated by the aperture size or the value of Ω_0 decreasing. But, when the size of the aperture is large enough, the effects of the aperture on the average intensity are too small to be measured.

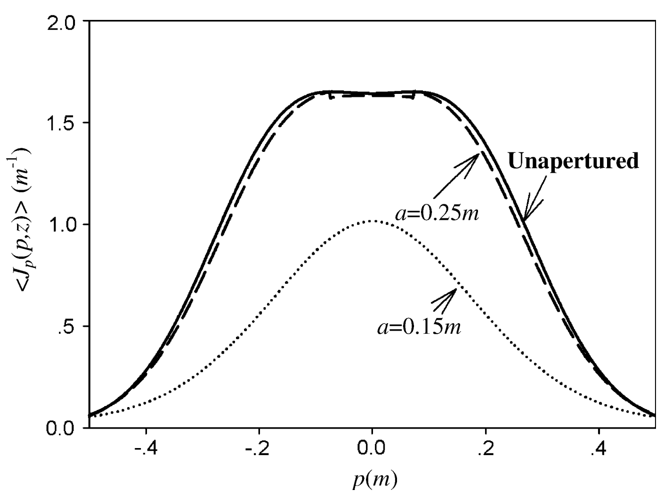

FIGURE 6 One-dimensional average normalized intensity distributions of a ChG beam with different radius of aperture at the z-plane, where $\Omega_0 = 30\ \mathrm{m}^{-1}$, $\lambda = 3.8 \times 10^{-6}$ m, $C_n^2 = 10^{-14}\ \mathrm{m}^{-2/3}$ and $z = 8 \times 10^3$ m

REFERENCES

1 L.W. Casperson, A.A. Tovar, J. Opt. Soc. Am. A **15**, 954 (1998)
2 L.W. Casperson, D.G. Hall, J. Opt. Soc. Am. A **14**, 3341 (1997)
3 A.A. Tovar, L.W. Casperson, J. Opt. Soc. Am. A **15**, 2425 (1998)
4 S. Yu, X. Fu, H. Guo, Opt. Commun. **13**, 203 (2002)
5 D. Zhao, H. Mao, H. Liu, J. Opt. A **6**, 77 (2004)
6 S. Yu, H. Guo, X. Fu, W. Hu, Opt. Commun. **204**, 59 (2002)
7 S. Konar, J. Soumendu, Opt. Commun. **236**, 7 (2004)
8 N. Zhou, G. Zeng, Opt. Commun. **232**, 49 (2004)
9 B. Lü, S. Luo, Opt. Commun. **178**, 275 (2000)
10 B. Lü, H. Ma, B. Zhang, Opt. Commun. **164**, 165 (1999)
11 X. Du, D. Zhao, Opt. Commun. **265**, 418 (2006)
12 Y. Baykal, J. Opt. Soc. Am. A **22**, 672 (2005)
13 Z.I. Feizulin, Y.A. Kravtsov, Radiophys. Quantum Electron. **10**, 33 (1967)
14 C.Y. Young, Y.V. Gilchrest, B.R. Macon, Opt. Eng. **41**, 1097 (2002)
15 J.C. Leader, J. Opt. Soc. Am. **68**, 175 (1978)
16 T. Shirai, A. Dogariu, E. Wolf, J. Opt. Soc. Am. A **20**, 1094 (2003)
17 H.T. Eyyuboğlu, Y. Baykal, Opt. Express **12**, 4659 (2004)
18 H.T. Eyyuboğlu, Y. Baykal, Appl. Opt. **44**, 976 (2005)
19 H.T. Eyyuboğlu, J. Opt. Soc. Am. A **22**, 1527 (2005)
20 H.T. Eyyuboğlu, Opt. Commun. **245**, 37 (2005)

21 Y. Cai, S. He, Opt. Express **14**, 1353 (2006)
22 C.H. Wang, M.A. Plonus, J. Opt. Soc. Am. **69**, 1297 (1979)
23 A. Ishimaru, Appl. Opt. **16**, 3190 (1977)
24 J.J. Wen, M.A. Breazeale, J. Acoust. Soc. Am. **83**, 1752 (1998)
25 Y. Zhang, Opt. Commun. **248**, 317 (2005)
26 I.S. Gradshteyn, I.M. Ryzhik, *Tables of Integrals, Series and Products* (Academic, New York, 1980)
27 Z. Mei, D. Zhao, J. Gu, Opt. Commun. **267**, 58 (2006)